Automatic Fetal Head Detection on Ultrasound Images by An Improved Iterative Randomized Hough Transform

Rong Xu, Jun Ohya
Graduate School of Global Information and Telecommunication Studies
Waseda University
Tokyo, Japan
xurong@fuji.waseda.jp

Bo Zhang[1], Yoshinobu Sato[2], Masakatsu G. Fujie[1]
[1]Faculty of Creative Science and Engineering
[1]Waseda University
[1]Tokyo, Japan
[2]Graduate School of Medicine
[2]Osaka University
[2]Osaka, Japan

***Abstract*—This paper describes an improved iterative randomized Hough transform (IRHT) method for automatic fetal head detection on ultrasound images. The traditional IRHT method iteratively updates a region of interest in the image space based on the latest ellipse parameters estimated by randomized Hough transform (RHT). The noise pixels are gradually excluded from the region of interest during the iteration process, and the estimation becomes progressively close to the target. However, owing to the absence of considering the number (*N*) of pixels on the ellipse, the parameters used to define the final detected ellipse are relatively volatile and the iteration is also unstable. For this reason, the result for each iteration in our improved IRHT method is selected as the detected ellipse with the maximal number of pixels on the ellipse, which is selected from the top-*M* peaks in the accumulators of the whole detected ellipse samples. The experiments on fetal ultrasound images demonstrate that the proposed method achieves more robust and accurate results, and has a better performance for fetal head detection than the traditional IRHT method.**

Keywords- fetal ultrasound image; fetal head detection; ellipse detection; iterative randomized Hough transform (IRHT)

I. INTRODUCTION

Fetal head detection and segmentation on ultrasound images is an important primary step for many clinical applications, such as fetal growth evaluation [1], gestational age estimation [2], fetal weight estimation [3], and obstetric diagnosis [4], etc. However, owing to the discontinuity and irregularity of fetal head skulls, low resolution and signal-to-noise ratio of ultrasound images, it is quite challenging for surgeons to recognize it manually, and also manual analysis is always time-consuming. Therefore, automated or semi-automated medical image processing [5-9] should be used to ensure a better effective, precise and consistent measurement.

Hough transform (HT) [10], Randomized Hough Transform (RHT) [11] and Random Sample Consensus (RANSAC) [12] are several typical techniques for ellipse detection, but they may fail when strong noise can corrupt the curve peaks in the parameter space. An novel method named iterative randomized Hough transform (IRHT) [8] was proposed for the detection of incomplete ellipses under strong noise conditions. Though the traditional IRHT method can detect an incomplete ellipse with strong noise successfully, its efficiency and accuracy can still be enhanced further. In this research, we introduce the number (*N*) of pixels on the ellipse, and propose an improved IRHT method for fetal head detection. Then, the result for each iteration in the improved IRHT method is selected as the detected ellipse with the maximal number of pixels on the ellipse, which is selected from the top-*M* peaks in the accumulators of the whole detected ellipse samples. The experiments on fetal ultrasound images demonstrate that the proposed method achieves more robust and accurate results, and has a better performance for fetal head detection than the traditional IRHT method.

The remaining paper is organized as follows: Chapter 2 introduces the improvements on pre-processing, the traditional IRHT method, and the improved IRHT method, Chapter 3 presents the experiments on fetal ultrasound images, and also provides the comparison of two methods, Finally, Chapter 4 gives a conclusion.

II. ALGORITHM

A. Pre-processing

For fetal head detection on ultrasound images, the skeletons of fetal head skulls should be extracted as the bright object in pre-processing. On the other hand, because speckle noise is often superimposed into ultrasound images, a bilateral filter [13] with a *5×5* window is exploited to reduce the speckle noise and preserve the edge by a nonlinear combination of nearby image values. Subsequently, a white top-hat transform in mathematical morphology is operated to increase the contrast through a *11×11* structuring element.

After that, the *K*-means clustering algorithm [14] is applied to distinguish the bright object on the fetal ultrasound image. In this way, the mean value μ_i and the standard deviation σ_i $(i = 1, \dots, k)$ of each cluster can be calculated from the segmentation results. Since the *K*-means method is sensitive to noise, the bright object separated from the segmentation results will be corrupted by much noise. On the other hand, we only need to extract the basic skeletons of fetal head skulls as the input of the IRHT method. Therefore, it is not essential to extract the whole bright object comprising much noise.

In order to suppress the noise impact in the *K*-means method, we make use of a global thresholding to convert the intensity image into a binary image, then the bright object can be extracted from the background by a simple operation that compares image gray values with a threshold value *T*. The following threshold value *T* verified in the experiments, is adapted to extract bright object,

$$T = \mu_{k-1} - 0.75 \times \sigma_{k-1} \tag{1}$$

where, μ_{k-1} is the mean value of the bright object, σ_{k-1} is the standard deviation of the bright object (Here, we suppose the bright object is classified into *k-1* cluster).

As for binary image, a binary morphologic opening operation with a *2×2* structuring element is used to remove some small bright objects. Morphologic dilation with a *1×1* structuring element and closure with a *2×2* structuring element are used to smooth the boundaries of the large bright objects. After a series of pre-processing, the skeletons of the bright object are extracted by distance transform [15].

B. Iterative randomized Hough transform

On ultrasound images, fetal head skulls often appear as the bright object with some gaps, because fetal head skulls are not completely closed. Besides, some other structures also may generate bright spots in an image. Furthermore, various artifacts and noise are usually present on ultrasound images. Consequently, a useful head detection algorithm must effectively deal with these disturbances. The iterative randomized Hough transform (IRHT) [8] was recently developed for the detection of ellipse with large gaps and strong noise, derived from randomized Hough transform (RHT) [11] method. The following items provide a brief description of the RHT algorithm and the IRHT algorithm.

1) Randomized Hough transform (RHT)

In a binary image, the curve to be detected can be modeled by $f(c, z) = 0$, where $c = [\alpha_1, \dots, \alpha_2]^t$ comprises *n*-dimensional parameters, $z = (x, y)$ represents the coordinates of pixels on the curve. The RHT method first randomly takes a sample of *n* pixels, $z_i = (x_i, y_i), i = 1, \dots, n$, and maps this sample into one point $c \in R^n$ in the *n*-D parameter space by solving a set of *n* equations $f(c, z_i) = 0$. If *c* is valid for ellipse, the counter at *c* is increased by one in the parameter space and stored in its corresponding accumulator. This process is repeated until a predefined number of valid samples (*K*) are processed. The location of the counter peak in the accumulators denotes a remarkable possibility of the curve in the image. For ellipse detection ($n = 5$), the following equation is suitable to be utilized [16, 17] :

$$x^2 + y^2 - U(x^2 - y^2) - V 2xy - Rx - Sy - T = 0 \tag{2}$$

where, the five parameters, $[U, V, R, S, T]^t$, can be converted into the standard ellipse parameters $c = [x_0, y_0, a, b, \phi]^t$, (x_0, y_0) are the center coordinates of the ellipse, a and b are its major and minor semi-axes, and ϕ is the angle of rotation, then the ellipse eccentricity is given by $e = b/a$ and

$$U = \cos 2\phi \frac{1 - e^2}{1 + e^2} \tag{3}$$

$$V = \sin 2\phi \frac{1 - e^2}{1 + e^2} \tag{4}$$

$$R = 2x_0(1 - U) - 2y_0 V \tag{5}$$

$$S = 2y_0(1 + U) - 2x_0 V \tag{6}$$

$$T = \frac{2a^2 b^2}{a^2 + b^2} - \frac{x_0 R}{2} - \frac{y_0 S}{2} \tag{7}$$

where, *U* and *V* depend only on ϕ and *e*. In particular, for a circle, *U* and *V* are zero.

2) Transform Formulas

In order to obtain the standard ellipse parameters $c = [x_0, y_0, a, b, \phi]^t$, we deduce the following formulas based on (3) – (7).

$$x_0 = \frac{SV + R + RU}{2(1 - U^2 - V^2)} \tag{8}$$

$$y_0 = \frac{RV + S - SU}{2(1 - U^2 - V^2)} \tag{9}$$

$$a = \sqrt{\frac{2T + x_0 R + y_0 S}{2(1 - \sqrt{U^2 + V^2})}} \tag{10}$$

$$b = \sqrt{\frac{2T + x_0 R + y_0 S}{2(1 + \sqrt{U^2 + V^2})}} \tag{11}$$

$$\phi = \frac{1}{2} \arctan \frac{V}{U} \tag{12}$$

3) Improved iterative randomized Hough transform

The IRTH method employs a randomized Hough transform (RHT) to a region of interest (ROI) in the image space by iterative parameter adjustment and reciprocal use of the image space and parameter space. In RHT method, the region of interest is always the whole image and it does not change during the whole process. However, the region of interest in the IRHT method is updated based on the latest estimates of parameters during the iteration process. At the same time, noise pixels are gradually excluded from the region of interest, and the estimation progressively becomes close to the target.

On the basis of the principle of the IRHT method, we further introduce the number (*N*) of pixels on the detected ellipse, and the detected ellipse with the maximal number of pixels on the ellipse, which is selected from the top-*M* peaks in the accumulators of the whole detected ellipse samples, is accepted as the result on each iteration for updating the region

of interest (Herein, *M* is selected as *10*). In addition, a slightly larger rectangular region is drawn as the ROI to compensate for the uncertainties in the detected ellipse. This iterative process continues until the size difference of the ROI between two iterations is very small, and the detected ellipse in the final iteration is the terminal result. Moreover, the convergence conditions in this process are as follows, less than 2.5° in ϕ; less than *2* pixels in each of x_0, y_0, a and b; and less than *6* pixels total in x_0, y_0, a and b.

III. EXPERIMENTS

Fetal ultrasound images are provided by Nanjing Maternity and Child Health Care Hospital in China, each of which has had prior consent from the Mother, before being used in this research. For the purpose of enhancing the performance of the algorithm, a priori information, reported by Hadlock et al. [2], is applied into this experiment, which shows that the eccentricity $e = b/a$ of the human fetal head has a mean (μ_e) of *0.783* and a standard deviation (σ_e) of *0.044*. It could be used to construct a constraint as $\mu_e - 3\sigma_e \le e \le \mu_e + 3\sigma_e$, namely, $0.651 \le e \le 0.915$, and about *99.7%* of fetal heads would have an eccentricity in this range.

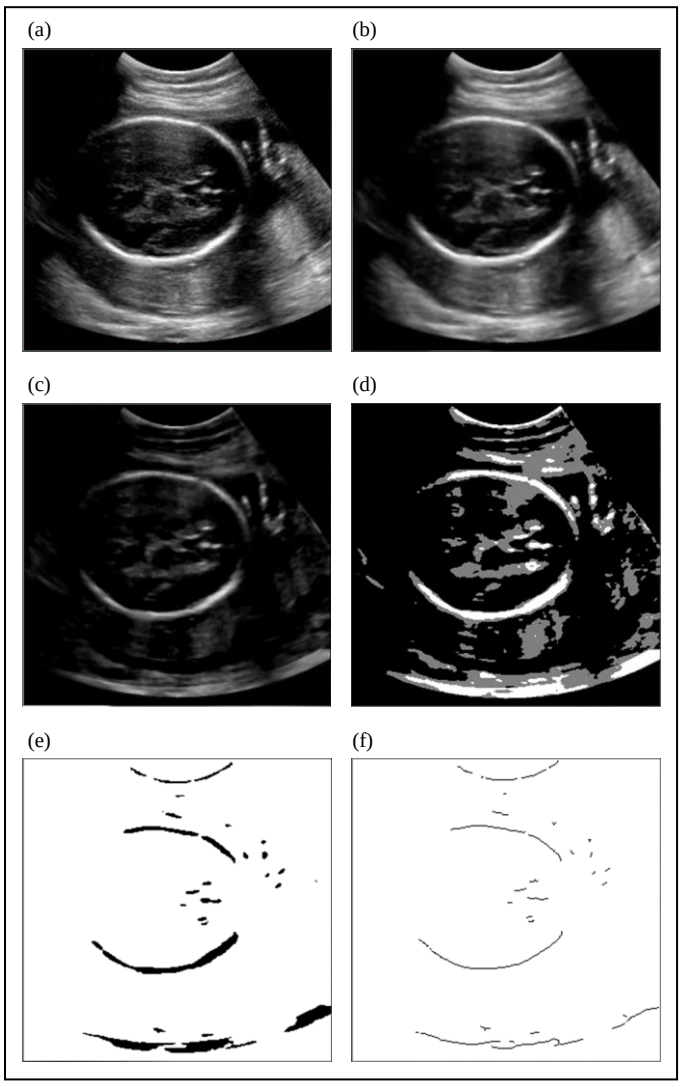

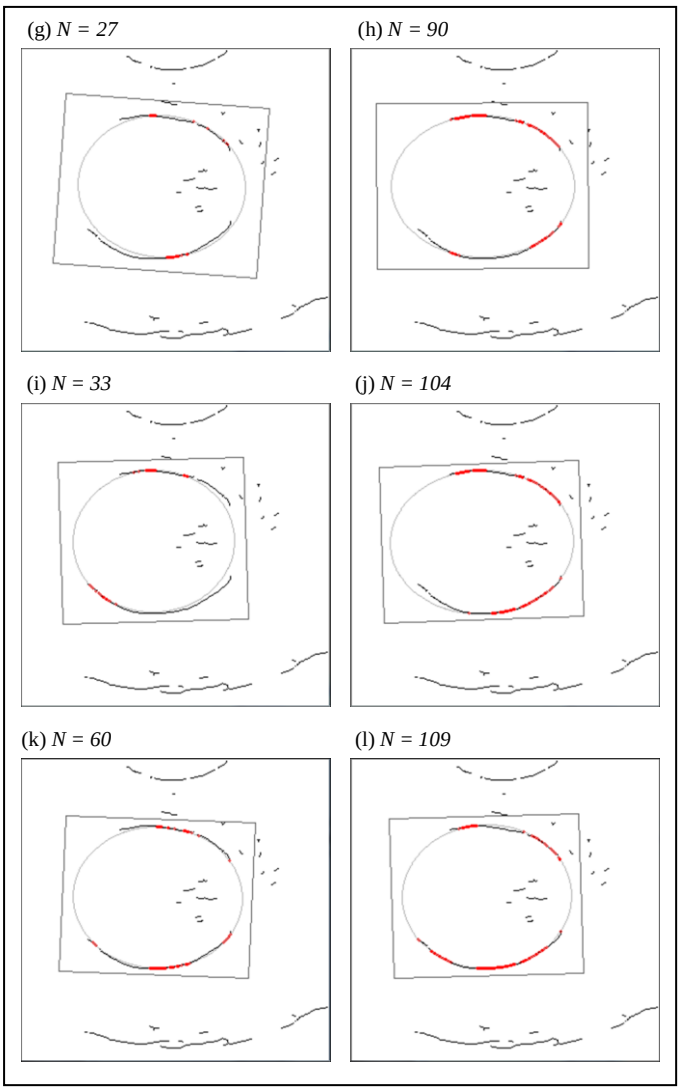

Figure 1. The Skeletonization and the detection of fetal head skulls on ultrasound images. (a) a clinical fetal ultrasound image; (b) the result of a bilateral filter with a *5×5* window on (a); (c) the result of a white top-hat transform with a *11×11* structuring element on (b); (d) the segmentation result of the *K*-means clustering method on (c); (e) the result of a global thresholding with a threshold value *T* defined in (1) on (d); (f) the skeletons of the bright object extracted by distance transform from (e); (g) the detected ellipse and ROI of the IRHT method after 1st iteration, where the red points denote the points on the detected ellipse, and the number of these red points is *N = 27* (the red points and *N* on the images from (g) to (l) are the same expression); (h) the detected ellipse and ROI of the improved IRHT method after 1st iteration, *N = 90*; (i) the detected ellipse and ROI of the IRHT method after 2nd iteration, *N = 33*; (j) the detected ellipse and ROI of the improved IRHT method after 2nd iteration, *N = 104*; (k) the final detected ellipse and ROI of the IRHT method after 13th iteration, *N = 60*; (l) the final detected ellipse and ROI of the improved IRHT method after 6th iteration, *N = 109*.

Fig. 1 describes the procedure of the skeletonization and the fetal head detection on fetal ultrasound images. As the results of each experiment are not the same, here we just choose a group of data closet to the average results listed in Table 1. In Fig. 1, (a) depicts a clinical fetal ultrasound image. (b) depicts the result of a bilateral filter with a *5×5* window on image (a). (c) depicts the result of a white top-hat transform with a *11×11* structuring element on image (b). (d) depicts the segmentation

Table 1. The comparison of the experimental results of *10* groups and the average results by the IRHT method and the improved IRHT method

Num	IRHT						
	x_0	y_0	a	b	ϕ (°)	T	N
1	135	138	83	71	4.71	8	99
2	134	140	84	69	2.64	7	56
3	133	140	83	70	1.00	28	51
4	132	137	86	70	-1.59	6	34
5	137	138	85	70	-3.04	36	41
6	131	138	86	72	4.23	19	41
7	135	138	80	71	4.08	10	107
8	131	138	82	71	2.56	5	56
9	135	139	88	71	4.39	3	68
10	136	138	85	71	-2.33	7	60
$\boldsymbol{\mu}$	134	138	84	71	1.67	**13**	**61**
$\boldsymbol{\sigma}$	*2.08*	*0.97*	*2.30*	*0.84*	*2.98*	*11.10*	*24.24*

Num	Improved IRHT						
	x_0	y_0	a	b	ϕ (°)	T	N
1	135	137	86	72	1.04	4	115
2	131	137	90	72	-1.18	18	91
3	135	137	87	72	-1.16	9	110
4	133	137	89	72	0.22	4	91
5	135	137	85	72	1.78	7	109
6	133	137	86	72	-1.15	3	84
7	135	138	87	71	1.16	6	109
8	132	138	90	71	0.33	2	94
9	134	137	88	72	1.16	3	92
10	131	137	90	72	0.00	3	90
$\boldsymbol{\mu}$	133	137	88	72	0.22	**6**	**99**
$\boldsymbol{\sigma}$	*1.65*	*0.42*	*1.87*	*0.42*	*1.09*	*4.77*	*10.97*

result of the *K*-means clustering method on image (c). (e) depicts the result of a global thresholding with a threshold value *T* defined in (1) on image (d). (f) depicts the skeletons of the bright object extracted by distance transform from image (e). (g), (i) and (k) depict the detected ellipses and ROIs (region of interest) after 1st, 2nd, and 13th iteration by the IRHT method (the detected ellipse after 13th iteration is the final result of the IRHT method), where the red points denote the points on the detected ellipse, and the numbers of these red points on each image are $N = 27$, $N = 33$, and $N = 60$. (h), (j), and (l) depict the detected ellipses and ROIs after 1st, 2nd, and 6th iteration through our improved IRHT method (the detected ellipse after 6th iteration is the final result of our method), where the red points denote the points on the detected ellipse, and the numbers of these red points on each image are $N = 90$, $N = 104$, and $N = 109$. Compared with the results of the IRHT method, the numbers of points on the detected ellipses of our method on each iteration are much larger, and at the same time the iteration of our method is also much smaller. Therefore, the results of our improved IRHT method are quite closer to the ground truth, and the efficiency is marginally better than that of the IRHT method.

Table 1 illustrates the comparison of the experimental results of *10* groups and the average results by the IRHT method and the improved IRHT method, where the last two lines list the mean value μ and the standard deviation σ averaged by the estimated parameters from these *10* groups. Among these data, we find the standard deviations σ of each estimated parameter by our improved IRHT method are all less than those of the IRHT method, which means the results of our method are more robust and consistent than the results of the IRHT method. Furthermore, *T* denotes the iteration of the algorithm, and its mean value, using our method is less than half of that value of the IRHT method, which means the efficiency of our method is greatly improved. *N* denotes the number of points on the detected ellipse, and its mean value of our method is nearly *1.5* times than that of the IRHT method, which also means the results of our method are more accurate than the results of the IRHT method.

IV. Conclusion

In this paper, we have proposed an improved iterative randomized Hough transform (IRHT) method for automatic fetal head detection on ultrasound images. Through the pre-processing based on the gray feature of ultrasound images, we could extract the basic skeletons of fetal head skulls and remove the noise maximally at the same time. To improve the efficiency and stability of the IRHT algorithm for the detection of incomplete ellipses with strong noise, we introduce the number of pixels on the ellipse and select the ellipse with the maximal number of pixels on the detected ellipse as the result on each iteration. The experiments on fetal ultrasound images demonstrate that the proposed method achieves more robust and accurate results, and has a better performance for fetal head detection than the traditional IRHT method.

Acknowledgment

Thanks to Nanjing Maternity and Child Health Care Hospital in China and the Mother, for allowing us to use these helpful ultrasound images for experiments. Also, the authors are grateful to the anonymous reviewers for their thorough reading, numerous valuable and constructive comments and suggestions to improve the presentation of this paper.

References

[1] F. P. Hadlock, "Ultrasound evaluation of fetal growth," In: Callen P, ed. Ultrasonography in obstetrics and gynecology, Philadelphia, PA: Saunders, pp. 129-142, 1988.

[2] F. P. Hadlock, R. Deter, R. Carpenter, and S. Park, "Estimating fetal age: Effect of head shape on bpd," American Journal of Roentgenology, vol. 137(1), pp. 83-85, 1981.

[3] I. Gull, G. Fait, J. Har-Toov *et al.*, "Prediction of fetal weight by ultrasound: The contribution of additional examiners," Ultrasound in Obstetrics and Gynecology, vol. 20(1), pp. 57-60, 2002.

[4] W. J. Zwiebel, and R. Sohaey, Introduction to ultrasound, PA: WB Saunders, Philadelphia, 1998.

[5] V. Salari, I. Zador, L. Chik, and R. Sokol, "Automated measurements of fetal head from ultrasound images," Medical Imaging IV: Image Processing, Newport Beach, CA, USA, vol. 1233, pp. 213-216, 1990.

[6] G. K. Matsopoulos, and S. Marshall, "Use of morphological image processing techniques for the measurement of a fetal head from

ultrasound images," Pattern Recognition, vol. 27(10), pp. 1317-1324, 1994.
[7] W. Lu, J. L. Tan, and R. Floyd, "Automated fetal head detection and measurement in ultrasound images by iterative randomized hough transform," Ultrasound in Medicine and Biology, vol. 31(7), pp. 929-936, 2005.
[8] W. Lu, and J. L. Tan, "Detection of ellipse in images with strong noise by iterative randomized hough transform (irht)," Pattern Recognition, vol. 41(4), pp. 1268-1279, 2008.
[9] Y. Shen, J. Yu, and Y. Wang, "Fetal skull analysis in ultrasound images based on iterative randomized hough transform," SPIE Medical Imaging 2009: Ultrasonic Imaging and Signal Processing, Lake Buena Vista, FL, vol. 7265, pp. 72650F, 2009.
[10] H. K. Yuen, J. Illingworth, and J. Kittler, "Detecting partially occluded ellipses using the hough transform," Image and Vision Computing, vol. 7(1), pp. 31-37, 1989.
[11] L. Xu, E. Oja, and P. Kultanen, "A new curve detection method - randomized hough transform (rht)," Pattern Recognition Letters, vol. 11(5), pp. 331-338, 1990.
[12] M. A. Fischler, and R. C. Bolles, "Random sample consensus - a paradigm for model fitting with applications to image analysis and automated cartography," Communications of the Acm, vol. 24(6), pp. 381-395, 1981.
[13] C. Tomasi, and R. Manduchi, "Bilateral filtering for gray and color images," Proceedings of the 1998 IEEE 6th International Conference on Computer Vision, Bombay, India, pp. 839-846, 1998.
[14] J. B. MacQueen, "Some methods for classification and analysis of multivariate observations," Proceedings of the 5th Berkeley Symposium on Mathematical Statistics and Probability, Berkeley, vol. 1, pp. 281-297, 1967.
[15] S. Chang, "Extracting skeletons from distance maps," International Journal of Computer Science and Network Security, vol. 7(7), pp. 213-219, 2007.
[16] V. F. Leavers, "The dynamic generalized hough transform - its relationship to the probabilistic hough transforms and an application to the concurrent detection of circles and ellipses," Cvgip-Image Understanding, vol. 56(3), pp. 381-398, 1992.
[17] A. Forbes, "Fitting an ellipse to data," National Physical Laboratory Report DITC 95/87, 1987.